FLOOD-PLAIN DELINEATION IN ICE JAM PRONE REGIONS

By Richard M. Vogel,[1] S. M. ASCE and Jery R. Stedinger,[2] A. M. ASCE

ABSTRACT: Flood-plain delineation in ice jam prone regions is in its infancy. A methodology is introduced for incorporating the risk of ice jams into flood-plain delineations in northern regions of the U.S. The distribution of flood elevations is derived from the marginal probability distributions for ice cover and storm induced (non-ice) flood elevations. An application indicates that incorporation of the hydraulics of an ice cover into flood-plain delineations can result in substantial increases in the inundation levels which generally implies a significant increase in the lateral extent of flood-plain boundaries. These results document the need to consider the probability of ice jam flood events in the computation of annual maximum flood elevation distributions and flood risk in ice jam prone regions.

INTRODUCTION

Flood-plain delineation has received considerable attention since the enactment of the National Flood Insurance Program. However, unique causes of flooding, such as ice jams, have not received sufficient attention and are not as well understood as storm induced, unobstructed floods. Recent advances in the field of ice engineering provide a variety of theoretical hydraulic models which characterize ice jam phenomena (12, 20,22,28,31). To evaluate the effect of ice jams on flood-plain delineations, the U.S. Army Corps of Engineers has incorporated a quasi-theoretical hydraulic model of ice jams into the HEC-2 Water Surface Profile Computer Program (12,33). Modification number 55 to the HEC-2 computer program (12), which contains the ice cover option, was released in March, 1982; a revised user's manual (33) documents the required input for the ice option. Calkins et al. (6) provide a description of the modified HEC-2 computer program along with a brief analysis of flow in fully and partially ice covered waterways. Although the ice cover option is a recent innovation, experience indicates that the model is a useful tool for predicting water surface elevations in ice covered natural stream channels (32).

This study illustrates a methodology for incorporating ice-jam phenomena into flood-plain studies. In northern regions of the U.S., where ice plays a significant role in the hydraulics of rivers, the distribution of flood events is comprised of at least two populations: annual maxima from ice jams and storm (non-ice) events. All further references to "storm" events refer to non-ice related flooding. The distribution of flood ele-

vations is a result of the probability distributions for both ice cover and storm induced flood elevations. A 16 mile reach along the Missisquoi River in northern Vermont was chosen to test the proposed methodology. Using the HEC-2 model, the marginal cumulative probability distributions of ice jam and storm induced flood elevations were estimated at 61 cross sections. The marginal cumulative probability distributions of ice jam and storm induced flood elevations were validated utilizing field surveys of actual flood events at selected sites along the 16 mile river reach. The total cumulative probability distribution for flood elevations can be computed from these two marginal distributions at each cross section.

Our results indicate that incorporation of the effect of ice jams into flood-plain delineations for the Missisquoi River would result in substantial increases in both the lateral extent of the flood-plain boundaries as well as the inundation levels. Ice jam flooding predominated in the distributions of flood elevations except in the vicinity of ice control structures, such as dams.

ICE JAMS

Ice jams are a well documented phenomenon which occur during the breakup of ice. Some recorded ice jams have been severe; the Yukon River, for example, rose 65 ft in the spring of 1930 to flood the village of Ruby (13). Water level rises of more than 20 ft are common when an ice jam is formed (20).

Most severe ice jams occur during the spring ice breakup. Investigations of the spring breakup phenomenon indicate that the breakup of ice on rivers is a complex function of precipitation, river discharge, wind, heat exchange, and other factors (20). The potential for an average winter ice cover on rivers in the U.S. may be represented approximately by 32° F spring isotherms in Fig. 1. The isotherms for February and March shown in Fig. 1 were interpolated from the Climatic Atlas of the U.S. (4) and are intended to provide an estimate of the likely extent of a winter ice cover on U.S. rivers and lakes. It is evident from Fig. 1 that a
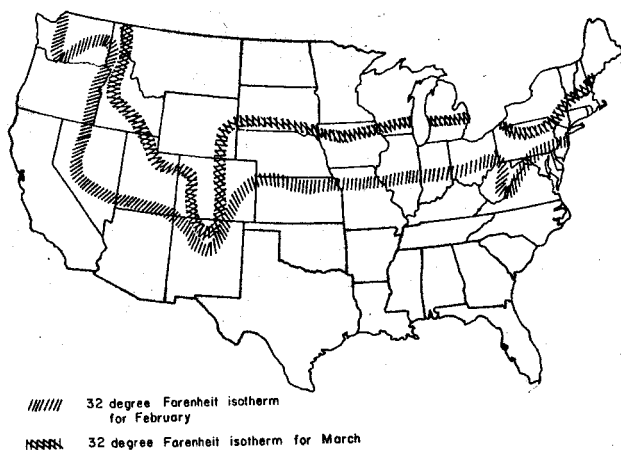

/////// 32 degree Farenheit isotherm
        for February

НЅЅЅ   32 degree Farenheit isotherm for March

FIG. 1.—32° F Spring Isotherms
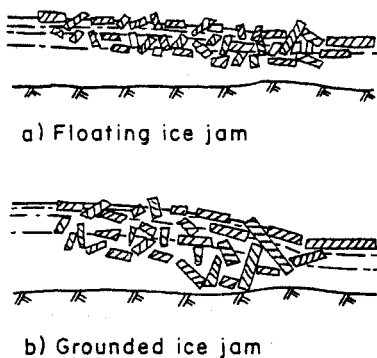
a) Floating ice jam

b) Grounded ice jam

FIG. 2.—Types of Ice Jams

substantial portion of U.S. rivers could maintain an ice cover for a limited time and are hence prone to ice jam phenomena. For example, the Susquehanna River in the vicinity of the Safe Harbor Hydropower Dam in southeastern Pennsylvania (approximately 32 mile upstream of its mouth at the Chesapeake Bay) is subject to semi-annual ice related flooding and the risk posed by ice is substantial; as observed in Ref. 1, "Ice related flooding which began on January 26 [1978] resulted in the highest water levels immediately upstream and downstream of the plant since the dam was constructed in 1931." Apparently flood elevations resulting from the ice cover in 1978 were in excess of those caused by Hurricane Agnes in 1972.

Ice jams are normally classified as either grounded or floating (Fig. 2). A floating jam may be initiated by the accumulation of ice floes in front of a solid ice cover. A floating jam's shape is nonuniform at the head and achieves a uniform thickness further upstream. Water flows freely beneath the accumulation of ice. A floating jam typically moves downstream by either an increase in river discharge or by the inflow of additional upstream ice. It may also melt in place. Although the mechanism of ice jam failure is fairly complex, the maximum water levels that can be reached are accessible to computation (22).

A grounded jam is formed by ice floes plunging to the streambed and being trapped between the streambed and the impeding solid ice cover. The obstacles which contribute to the formation of a grounded jam are the existing ice cover, streambed irregularities, and changes in hydraulic conditions. The grounded jam generally plugs the entire river cross section, causing an "ice dam." The occurrence of a grounded jam is difficult to predict unless sufficient field data exist to describe its nature and the causes of its occurrence.

THEORETICAL ICE COVER MODEL

The state of the art of ice jam modeling appears to preclude the analysis of grounded jams due to their inherently unpredictable nature. This study concentrates on the effect of the more common floating jams. A variety of mathematical hydraulic models have been developed to simulate the behavior of a mass of detached floating ice floes as depicted in Fig. 2(a). Several computational models which incorporate the me-

chanics of a floating ice cover with a step-backwater hydraulic routine for open channel flow have been developed, but few are available for public use. Petryk et al. (19) have developed a quasi-dynamic model which simulates the ice cover buildup and its subsequent decay in river channels. Their model consists of backwater computations to satisfy the hydraulic constraints, heat balance calculations to evaluate the volume of frazil ice generated as well as the major melting effects, and four ice stability constraints to evaluate changes in ice cover thickness. Clement and Petryk (7) provide a detailed discussion of the advantages and limitations of their model.

The U.S. Army Corps of Engineers Hydrologic Engineering Center and Cold Regions Research and Engineering Laboratory have recently incorporated into their step-backwater hydraulic model, HEC-2 (12,33) the hydraulics of floating ice. Their model consists of the standard HEC-2 model modified to account for a mass of floating ice which is characterized by its thickness, density, and roughness coefficient. The theoretical model is based upon the fundamental assumptions of gradually varied steady flow with the head loss between cross sections given by the uniform flow equation. It is evident that the accuracy of this theoretical model is highly dependent upon assumptions regarding the resistance to flow caused by the ice cover as well as variations in the width, thickness, and type of ice cover, in addition to the assumptions regarding the mechanics of the ice cover thickening process.

The ice cover is incorporated into the HEC-2 computer program through a modification in the HEC-2 bridge code. Floating ice is handled as if it was a floating bridge. Standard techniques are employed to determine the area blocked by a bridge deck and the additional wetted perimeter caused by a submerged low chord. Input data requirements are identical to the standard HEC-2 requirements with the addition of ice cover data. The model utilizes the Belokon-Sabaneev formula (26) to determine a composite Mannings n value for the channel, overbank areas and ice cover. The ice cover roughness coefficient can be input for each section, but a composite value must be used to characterize the ice cover roughness at each cross section. Ice cover thickness is input at each section allowing for different values in the channel and overbank areas. Use of the HEC-2 hydraulic model requires further information regarding the winter flow regime as well as the channel geometry.

MODEL APPLICATION AND VALIDATION

Ice jams are known to be extremely complex dynamic phenomena. However, Vogel and Root (32) showed that excellent agreement may be obtained between field verified ice jam flood stages and simulated ice jam flood stages using HEC-2 (12). Based on solid ice thickness values estimated from air temperature records in conjunction with Michel (20), Vogel and Root chose to employ a constant and uniform ice thickness of 2.0 ft for both channel and overbank regions and a constant roughness coefficient for the underside of the ice cover of 0.057 throughout the 16 mile reach. Actual measurements of ice jam thickness were not available for this reach. While the procedure adopted by Vogel and Root

performed adequately in this instance, field measurements of ice thickness should be used when available.

Using U.S. Geological Survey discharge estimates recorded for: (1) The worst ice jam on record (March 6, 1979); and (2) an average annual ice jam event, Vogel and Root computed the likely flood stages along the entire 16 mile reach. At four documented ice jam sites, actual ice jam flood stages were field-surveyed using newspaper articles, photographs, and interviews with long-time residents to obtain appropriate flood marks. Excellent agreement was obtained between those field surveyed flood elevations and the simulated flood elevations using constant ice thickness and ice roughness values. In addition, the simulated flood elevations at each of the 61 cross sections were delineated on topographic maps and the lateral extent of flooding was discussed at town meetings with local flood-plain residents. This validation process, which is mandated by the Federal Emergency Management Agency during the course of any Flood Insurance Study, served to further validate the model over this particular river reach.

COMPOSITE DISTRIBUTION FUNCTION

In northern regions of the U.S., the distribution of maximum annual flood elevations depends on both the distributions of ice jam and storm induced flood elevations. Consider first, the marginal cumulative distribution functions $F_i(h_i)$ and $F_s(h_s)$ of ice jam flood elevations h_i, and storm induced flood elevations h_s, respectively. Given the marginal probability density functions (pdf) for ice jam flood elevations $f_i(h_i)$ and storm induced flood elevations $f_s(h_s)$ the corresponding marginal cumulative probability functions (cdf) for both classes of events can be computed from the relationships

$$F_i(h_i) = \int_{-\infty}^{h_i} f_i(h_i')\,dh_i'\,; \quad\dots\dots\dots\dots\dots\dots\dots\dots\dots\dots\dots\dots\dots\dots \quad (1)$$

$$\text{and}\quad F_s(h_s) = \int_{-\infty}^{h_s} f_s(h_s')\,dh_s' \quad\dots\dots\dots\dots\dots\dots\dots\dots\dots\dots\dots\dots\dots \quad (2)$$

Most severe storm induced floods are caused by convective storms which generally occur during the summer months. Severe ice jams usually occur during the spring breakup and melting process. Hence, severe storm events may be considered to be independent of the severe ice jam events. The matter of independence is complicated by the fact that some ice jams are the result of both frontal storm activity and the spring breakup of ice.

The aim here is to determine the cdf of the annual maximum flood elevation h_m, given by

$$h_m = \max{(h_i, h_s)} \dots\dots\dots\dots\dots\dots\dots\dots\dots\dots\dots\dots\dots\dots\dots\dots\dots\dots \quad (3)$$

The cdf of h_m, denoted as $F_m(h_m)$, is found by integrating the joint pdf of h_i and h_s over the region where the maximum of both h_i and h_s is less than h_m

$$F_m(h_m) = P[\max(h_i, h_s) < h_m] = \int_{-\infty}^{h_m} \int_{-\infty}^{h_m} f_{i,s}(h_i, h_s) \, dh_i \, dh_s \dots \dots \dots \dots \quad (4)$$

Assuming that the annual maximum ice jam flood elevation h_i and the annual maximum storm induced flood elevation h_s are independent, we obtain

$$F_m(h_m) = \int_{-\infty}^{h_m} f_i(h_i) \, dh_i \int_{-\infty}^{h_m} f_s(h_s) \, dh_s \dots \dots \dots \dots \dots \dots \dots \quad (5)$$

Thus the probability that both h_i and h_s are less than h_m is given by

$$F_m(h_m) = F_i(h_m) F_s(h_m) \dots \dots \dots \dots \dots \dots \dots \dots \dots \dots \dots \dots \quad (6)$$

Benjamin and Cornell (3) consider a similar situation.

HYDROLOGY

Simulation of the water surface profiles requires information regarding the probability distributions of peak annual discharges for storm induced floods and peak winter discharges for ice jam induced floods. This study uses discharge measurements from the U.S.G.S. gage on the Missisquoi River near East Berkshire (#04293500) over a 45 year period. For storm induced floods, a Log Pearson Type III distribution was fitted to the 45 yr annual series according to the Water Resources Council guidelines (10). For ice jam floods, a Log Pearson Type III distribution was also fitted using the at-site skew coefficient to the 45 yr series of annual peak discharges during the potential ice jam season. The potential ice jam season is taken to be from December 1 until March 31. Discharge quantiles from each of the distributions are given in Table 1. Storm discharges are approximately twice the magnitude of the ice jam discharges at each recurrence interval. The fact that the storm season overlaps the ice jam season does not bias the results here; extreme floods, with a recurrence interval greater than five years occurred only during the summer months.

Should the overlap between the storm and ice season cause problems, then in deriving the distribution of maximum annual discharges for storm events, one's analysis should be restricted to only those flood flows which did not occur during the ice jam season. The resulting distribution of storm event discharges should be fairly independent of the distribution of ice jam discharges and the two marginal distributions can be combined using Eq. 6.

TABLE 1.—Comparison of Ice Jam and Storm Discharge Estimates, in Cubic Feet per Second

	Recurrence Interval	
Season (1)	10 year (2)	100 year (3)
Ice jam	12,900	17,500
Storm	22,400	34,000

The probability distributions for storm event discharges can be converted into the corresponding distributions for flood elevations using HEC-2. As this is a very involved operation, an approximate procedure was employed. HEC-2 was used to derive the 10- and 100-yr flood elevation at each cross section then a two parameter lognormal distribution was used to interpolate the elevation of floods corresponding to other recurrence intervals. The fitted lognormal probability density function for storm event flood elevations is of the form

$$f_s(h_s) = \frac{1}{\sigma h_s \sqrt{2\pi}} \exp \left\{ -\frac{1}{2\sigma^2} [\ln (h_s) - \mu]^2 \right\} \dots \dots \dots \dots (7)$$

for $h_s > 0$.

The required mean μ and standard deviation σ of the logarithms of h_s are given by

$$\sigma = \ln \frac{\left[\dfrac{h_s^{(0.99)}}{h_s^{(0.9)}} \right]}{(z_{0.99} - z_{0.9})} \dots \dots \dots \dots \dots \dots \dots (8)$$

and $\quad \mu = \ln [h_s^{(0.9)}] - \sigma z_{0.9} \dots \dots \dots \dots \dots \dots (9)$

in which z_p is the $100p$ percentile of a standard-normal distribution and $h_s^{(0.9)}$ and $h_s^{(0.99)}$ are the 10-yr and 100-yr storm induced flood elevations.

The same procedure was used to obtain a lognormal distribution describing the probability distribution of ice jam induced flood elevations. In this latter case, the 10-yr and 100-yr ice jam induced flood elevations are larger than those flood elevations that would occur due to the projected spring floods in the absence of ice jams.

If a two-parameter lognormal distribution failed to provide an adequate approximation to the indicated distributions, one could use three quantiles of the flood elevation distributions and fit a three-parameter lognormal distribution or other distributions which are convenient for such tasks.

RESULTS

Use of a lognormal model to describe the marginal distributions of ice jam and storm induced flood elevations in conjunction with Eq. 6 allows determination of the annual maximum flood-elevation frequency distribution. This was done at 61 cross sections on the Missisquoi River. Figs. 3 and 4 show the differences between $F_m(h_m)$, $F_i(h_m)$ and $F_s(h_m)$ by comparing the 10-yr and 100-yr flood elevations for each distribution. To avoid confusion which might be caused by channel morphology, flood elevations at each cross section are measured in both figures relative to the 100-yr flood elevation of the estimated annual maximum composite flood distribution $F_m(h_m)$.

Naturally, the flood elevations corresponding to any recurrence interval for the annual maximum flood distribution is never less than the corresponding flood elevation quantiles of the ice jam and storm in-
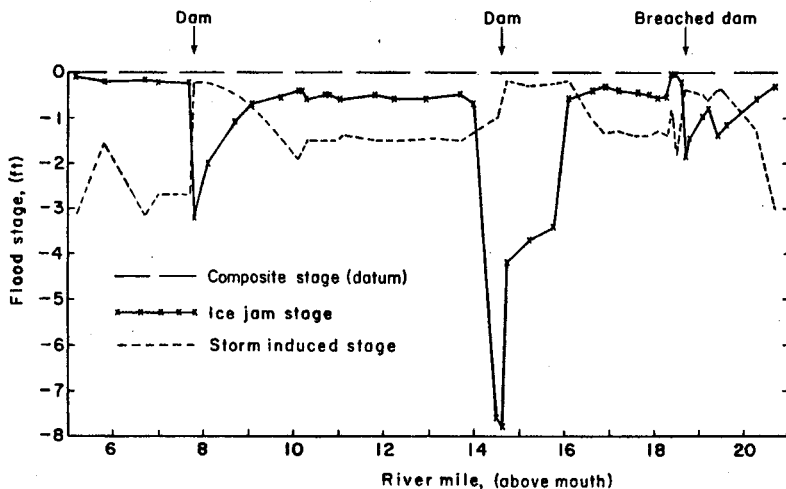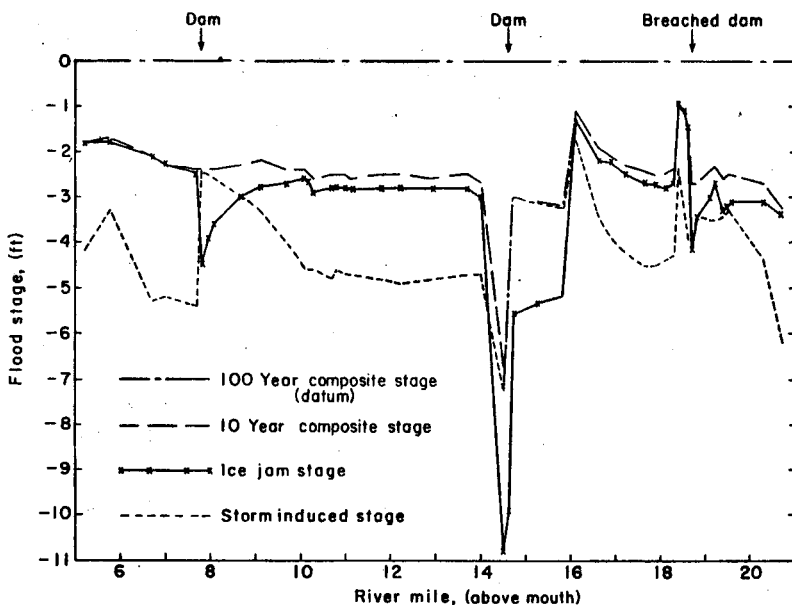
FIG. 3.—Plot of Flood Stages for 100-Yr Event

FIG. 4.—Plot of Flood Stages for 10-Yr Event

duced flood distributions. Only if the effect of one of the two marginal distributions is negligible do the quantiles of the annual maximum distribution equal the corresponding quantiles of the dominant marginal flood elevation distribution. This situation is approached in only a few places: between river miles 18 and 19 and perhaps between river miles five and eight. Elsewhere, both causes of extreme flood elevations contribute to the overall flood hazard as described by $F_m(h_m)$. However, of the two causes of flooding, ice jams were the predominant or more important factor, except in the vicinity of the three dams. In general, the 10-yr and 100-yr ice jam induced flood elevations were larger than the corresponding storm induced flood elevations except in the vicinity of the dams. Moreover, the relatively small difference between the ice jam
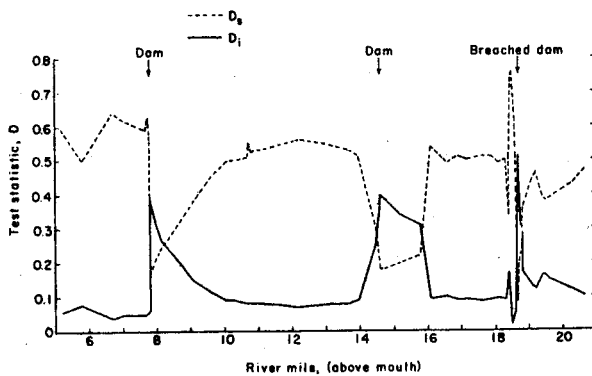
213

FIG. 5.—Plot of Kolmogorov-Smirnoff Test Statistics

flood elevations and annual maximum flood elevations at several places documents the importance of ice jam flooding at those points. However, storm events were the predominant factors near dams.

An objective measure of the difference between the individual distributions, $F_i(h_m)$ and $F_s(h_m)$, when compared to the annual maximum distribution for flood elevations, $F_m(h_m)$, is provided by the Kolmogorov-Smirnoff statistic. To evaluate the relative difference between a marginal lognormal distribution for ice jam flood elevations and the annual maximum or composite flood elevation distribution one may use

$$D_i = \max_{0 \le h_m \le \infty} |F_i(h_m) - F_m(h_m)| \dots\dots\dots\dots\dots\dots\dots\dots\dots\dots \quad (10)$$

Similarly, to evaluate the difference between the marginal lognormal distribution of storm induced flood elevations and the composite flood elevation distribution one may use

$$D_s = \max_{0 < h_m < \infty} |F_s(h_m) - F_m(h_m)| \dots\dots\dots\dots\dots\dots\dots\dots\dots\dots \quad (11)$$

D is the greatest difference between the two cumulative distribution functions. The greater the value of D, the greater the difference between the two distributions. It is emphasized that the D statistic is used here simply as an objective measure of relative difference rather than for the purpose of hypothesis testing.

Fig. 5 shows the values of D_i and D_s at each of the 61 cross sections. In general, the D_i values are less than the D_s values, except in the vicinity of the three dams. Interestingly, the D_i and D_s curves are approximately mirror images of each other: the peaks of one correspond to the troughs of the other. The transition regions, where storm events are the more important factor in determining flood risk, extend from the tailwater of each dam to a section upstream where the dams no longer exert hydraulic control.

FLOOD HAZARD

Present flood-plain management practices often make use of flood elevations corresponding to events with 10- and 100-yr recurrence intervals. The National Flood Insurance Program defines a "flood hazard fac-
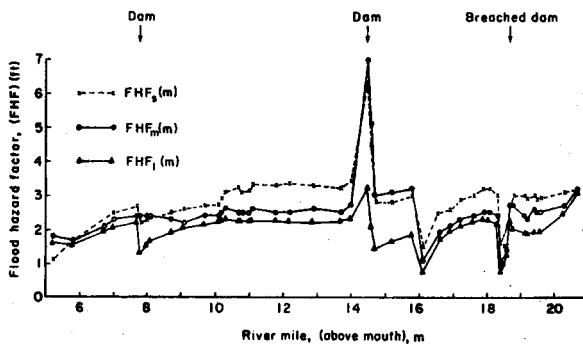
FIG. 6.—Plot of Flood Hazard Factors

tor'' (FHF) as the difference between the 10- and 100-yr flood elevations at each cross section.

Consider the flood hazard factor for storm events, ice jam events and both. Let

$$\text{FHF}_s(m) = h_s^{(0.99)} - h_s^{(0.9)} \dots \dots \dots \dots \dots \dots \dots \dots \dots \dots \dots \dots \quad (12)$$

$$\text{FHF}_i(m) = h_i^{(0.99)} - h_i^{(0.9)} \dots \dots \dots \dots \dots \dots \dots \dots \dots \dots \dots \dots \quad (13)$$

$$\text{FHF}_m(m) = h_m^{(0.99)} - h_m^{(0.9)} \dots \dots \dots \dots \dots \dots \dots \dots \dots \dots \dots \dots \quad (14)$$

in which $\text{FHF}_s(m)$, $\text{FHF}_i(m)$, and $\text{FHF}_m(m)$ correspond to the flood hazard factors for storm induced, ice induced and composite or annual maximum flood elevations at river mile m. Large values of FHF(m) indicate low flood hazard while small values indicate high hazards. The flood hazard factors are a descriptor of the relationship between inundation levels and flood risk. Large values of FHF indicate that the severity of flooding increases rapidly with flood recurrence interval; small values indicate that inundation levels are similar for both 10- and 100-yr flood events.

The flood hazard factor functions are displayed in Fig. 6. It is apparent that $\text{FHF}_i(m)$ is smaller than $\text{FHF}_s(m)$ above river mile 5.8. This reflects the observations of local residents that ice jam flooding occurs every year and the worst ice jam flood of record was only one to two feet higher than annual ice jam floods.

A weighted flood hazard factor ($\overline{\text{FHF}}$) for a reach is usually computed to determine appropriate actuarial insurance premiums for structures within the reach. For the 15.5 mile reach along the Missisquoi River

$$\overline{\text{FHF}} = \frac{1}{15.5} \int_{5.2}^{20.7} \text{FHF}(m)\, dm \dots \dots \dots \dots \dots \dots \dots \dots \dots \dots \dots \quad (15)$$

The computed $\overline{\text{FHF}}$ for ice jam, composite, and storm induced flooding are 1.8, 2.5, and 2.9 ft respectively. Thus incorporation of ice jams into flood frequency calculations decreases the average flood hazard factor from 2.9 ft to 2.5 ft, indicating increased average flood hazard.

SUMMARY

The National Flood Insurance Program is developing flood-plain maps with associated risk zones at approximately 20,000 locations in the United

States (2). The scale and cost of the program in conjunction with the vested interests which form during and after each study often preclude significant modification of flood-plain boundary delineations or insurance rate structures or both after studies are completed. Thus if flood-plain delineations and insurance rate structures are to be economically efficient and hydrologically accurate, it is important that such studies include all important causes of flooding and make use of the best available statistical techniques.

Past and recent research has identified weaknesses and potential problems with traditional flood-flow frequency estimation techniques. Beard (2) has emphasized that traditional procedures provide a downward biased estimate of flood risk. Hardison and Jennings (11) show that this downward bias in estimated flood risk given by the traditional procedures yield poor estimates of expected flood losses. Stedinger (27) discusses these issues and their relationship to Bayesian flood frequency estimation procedures. Even ignoring that issue, considerable difference of opinion exists as to how one can best fit Log Pearson Type 3 distributions to flood flow data (16,17,18,21,25). Moreover, relatively recent work has shown that much can be gained by use of regional information (besides use of log skewness) when estimating particular quantiles of the flood flow frequency distribution even at gaged sites (14,15,29,30). Of course, all of these methods, and those in this paper, are dependent on measured or reported flood discharge values; Potter and Walker (24) perceptively point out that these estimates are subject to measurement error with the largest errors generally associated with the large flood flows, those flows of primary interest here.

There is more to flood-plain delineation than estimating the discharge distribution for free-flowing storm events. Discharge values must be converted into stages; the uncertainty inherent in that process has been examined by Burges (4). A nationwide survey of the accuracy of 100-yr flood-plain delineations has been performed by Burkham (5).

The analysis herein has derived the approximate distributions of annual maximum flood elevations resulting from both storm events and ice jam events. In the example, the distributions of ice jam induced flood elevations were found to be more important than those for storm events in determining the risk of flooding at all locations along the 15.5 mile reach of the Missisquoi River except in the vicinity of three dams. Incorporation of the derived marginal distribution of the ice jam induced flood elevations to estimate the distribution of annual maximum flood elevations results in substantial increases in both the lateral extent of flood-plain boundaries as well as inundation levels for both the 10- and 100-yr events.

The results of this study indicate the importance of incorporating the effects of ice jams in flood-plain delineations along the Missisquoi River. It is likely that other studies in northern ice prone regions will further document the need to incorporate ice jam flood events into the computation of annual maximum flood elevation distributions and flood risk in general. The Federal Emergency Management Agency (9) has recently acknowledged the importance of, and provided guidance for, the incorporation of ice cover hydraulics into flood-plain delineations in ice jam prone regions.

APPENDIX I.—REFERENCES

1. *A Study of the Ice Jam Problem at the Safe Harbor Hydroelectric Project*, prepared by Harza Engineering Corp., Safe Harbor Water Power Corp., July, 1981.
2. Beard, L. R., "Impact of Hydrologic Uncertainties on Flood Insurance," *Journal of the Hydraulics Division*, ASCE, Vol. 104, No. HY11, 1978, pp. 1473–1484.
3. Benjamin, J. R. and C. A. Cornell, *Probability, Statistics and Decision for Civil Engineers*, McGraw-Hill Book Co., New York, N.Y., pp. 114–115, 1970.
4. Burges, S. J., "Analysis of Uncertainty in Flood Plain Mapping," *Water Resources Bulletin*, Vol. 15, No. 1, 1979, pp. 227–243.
5. Burkham, D. E., "Accuracy of Flood Mapping," Journal of Research of the United States Geological Survey, Vol. 6, No. 4, 1978, pp. 515–527.
6. Calkins, D. J., Hayes, R., Daly, S. F., and Montalvo, A., "Application of HEC-2 for Ice-Covered Waterways," *Journal of the Technical Councils of ASCE*, ASCE, Vol. 108, No. TC2, Nov., 1982.
7. Clement, F. C., and Petryk, S., *Limitations to Numerical Modeling of Ice in Rivers: Proceedings of the Workshop on Hydraulic Resistance of River Ice*, Canada Center for Inland Waters, Burlington, Ontario, Sept., 1980.
8. *Climatic Atlas of the United States*, Environmental Data Service, U.S. Dept. of Commerce, June, 1968.
9. *Guidelines and Specifications for Study Contractors*, Federal Emergency Management Agency, Sept., 1982.
10. *Guidelines for Determining Flood Flow Frequency*, Bulletin 17B, Hydrology Committee, U.S. Water Resources Council, revised Sept., 1981.
11. Hardison, C. H., and Jennings, M. E., "Bias in Computed Flood Risk," *Journal of the Hydraulics Division*, ASCE, Vol. 98, No. HY3, 1972, pp. 415–427.
12. *HEC-2 Water Surface Profiles*, Generalized Computer Program, U.S. Army Corps of Engineers, Hydrologic Engineering Center, Davis, Calif., Nov., 1976, (Modification 55 for Ice Cover Analysis, released March 29, 1982).
13. Henry, W. K., "The Ice Jam Floods of the Yukon River," *Weatherwise*, Vol. 18, No. 2, 1965, pp. 81–85.
14. Kuczera, G., "Combining Site-Specific and Regional Information: An Empirical Bayes Approach," *Water Resources Research*, Vol. 18, No. 2, 1982, pp. 306–314.
15. Kuczera, G., "Robust Flood Frequency Models," *Water Resources Research*, Vol. 18, No. 2, 1982, pp. 315–324.
16. Landwehr, J. M., Matalas, N. C., and Wallis, J. R., "Some Comparisons of Flood Statistics in Real and Log Space," *Water Resources Research*, Vol. 14, No. 5, 1978, pp. 902–920.
17. Lettenmaier, D. P., and Burges, S. J., "Correction for Bias in Estimation of the Standard Deviation and Coefficient of Skewness of the Log Pearson 3 Distribution," *Water Resources Research*, Vol. 16, No. 4, 1980, pp. 762–766.
18. McCuen, R. H., "Map Skew???," *Journal of the Water Resources Planning and Management Division*, ASCE, Vol. 105, No. WR2, Sept., 1979, pp. 269–277.
19. McCuen, R. H., "Map Skew???," Closure, *Journal of the Water Resources Planning and Management Division*, ASCE, Vol. 107, No. WR2, 1981.
20. Michel, B., "Winter Regime of Rivers and Lakes," *Cold Regions Science and*

Engineering Monograph 111-B1a, U.S. Army Corps of Engineers, Hanover, N.
1971.

21. Nozdryn-Plotnicki, M. J., and Watt, W. E., "Assessment of Fitting Te
niques for the Log Pearson Type 3 Distribution using Monte Carlo Sim
tion," *Water Resources Research,* Vol. 15, No. 3, 1979, pp. 714–718.
22. Pariset, E., Hausser, R., and Gagnon, A., "Formation of Ice Covers and
Jams in Rivers," *Journal of the Hydraulics Division,* ASCE, Vol. 2, No. H
pp. 1–24.
23. Petrk, S., Panu, U. S., Kartha, V. C., and Clement, F., "Numerical Model
and Predictability of Ice Regime in Rivers," *Proceedings of the IAHR, Inter
tional Symposium on Ice,* Quebec, Canada, 1981, pp. 426–435.
24. Potter, K. W., and Walker, J. F., "A Model of Discontinuous Measurem
Error and Its Effects on the Probability Distribution of Flood Discharge M
surements," *Water Resources Research,* Vol. 17, No. 5, 1981, pp. 1505–150
25. Rao, D. V., "Log Pearson Type 3 Distribution: Method of Mixed Moment
Journal of the Hydraulics Division, ASCE, Vol. 106, No. HY6, 1980, pp. 9!
1019.
26. Sabaneev, A. A., "On the Computation of a Uniform Flow in a Channel w
Non-Uniform Walls" (in Russian), *Transactions,* Leningrad Polytechnical
stitute, No. 5, 1948.
27. Stedinger, J. R., "Design Events with Specified Flood Risk," *Water Resour
Research,* Vol. 19, No. 2, 1983, pp. 511–522.
28. Tatinclaux, J. C., "Equilibrium Thickness of Ice Jams," *Journal of the Hydra
ics Division,* ASCE, Vol. 103, No. HY9, 1977, pp. 959–974.
29. Tung, Y-K, and Mays, L. W., "Reducing Hydrologic Parameter Unc
tainty," *Journal of the Water Resources Planning and Management Division,* ASC
Vol. 107, No. WR1, 1981, pp. 245–262.
30. Tung, Y-K, and Mays, L. W., "Reducing Hydrologic Parameter Uncertain
Errata," *Journal of the Water Resources Planning and Management Division,* ASC
Vol. 107, No. WR2, pp. 588–589.
31. Uzuner, M. S., and Kennedy, J. F., "Theoretical Model of River Ice Jam:
Journal of the Hydraulics Division, ASCE, Vol. 102, No. HY9, 1976, pp. 136
1383.
32. Vogel, R. M., and Root, M. J., "The Effects of Floating Ice Jams on the Ma
nitude and Frequency of Floods Along the Missisquoi River in Northern V
mont," *Proceedings of the IAHR, International Symposium on Ice,* Quebec, Ca
ada, 1981, pp. 347–360.
33. *Water Surface Profiles—User's Manual,* HEC-2, U.S. Army Corps of Enginee
Hydrologic Engineering Center, Sept., 1982.

APPENDIX II.—NOTATION

The following symbols are used in this paper:

D_i = Kolmogorov-Smirnoff test statistic for ice jams;
D_s = Kolmogorov-Smirnoff test statistic for storm induce
floods;
$F_i(h_i)$ = cumulative probability function for ice jam flood elevatior
$F_s(h_s)$ = cumulative probability function for storm induced floc
elevations;
$F_m(h_m)$ = composite cumulative probability function for annu
maximum flood elevation;
$\overline{\text{FHF}}$ = weighted flood hazard factor;
$\text{FHF}_i(m)$ = flood hazard factor for ice jam floods at river mile *n*
$\text{FHF}_s(m)$ = flood hazard factor for storm induced floods at rive
mile *m*;

$\text{FHF}_m(m)$ = flood hazard factor for annual maximum flood at river mile m;

$f_i(h_i)$ = probability density function for ice jam flood elevations;

$f_s(h_s)$ = probability density function for storm induced flood elevations;

$f_{i,s}(h_i, h_s)$ = joint probability density function for ice jam and storm induced flood elevations;

h_m = annual maximum flood elevation;

$h_i^{(p)}$ = ice jam flood elevation with non-exceedance probability p;

$h_s^{(p)}$ = storm induced flood elevation with nonexceedance probability p;

$h_m^{(p)}$ = annual maximum or composite flood elevation with non-exceedance probability p;

m = miles above river mouth;

z_p = $100p$ percentile of standard normal distribution;

σ = standard deviation of transformed flood elevation; and

μ = mean of transformed flood elevation.